Eur J Nucl Med Mol Imaging (2008) 35:379–385
DOI 10.1007/s00259-007-0610-3

ORIGINAL ARTICLE

In vivo biodistribution of an androgen receptor avid PET imaging agent 7-α-fluoro-17 α-methyl-5-α-dihydrotestosterone ([^{18}F]FMDHT) in rats pretreated with cetrorelix, a GnRH antagonist

Sudha Garg · Aniruddha Doke · Kimberly W. Black · Pradeep K. Garg

Received: 17 July 2007 / Accepted: 16 September 2007 / Published online: 13 October 2007

Abstract
Purpose For this study, we have assessed the in vivo distribution and androgen receptor (AR) seeking properties of an F-18-labeled androgen [^{18}F]FMDHT in rats castrated with a GnRH antagonist.
Materials and methods The radiochemical synthesis of [^{18}F]FMDHT was performed using a previously published method. The radiochemical synthesis provided the desired product in good radiochemical yields and radiochemical purity. In vivo biodistribution studies were performed in chemically castrated rats. The animals were castrated using cetrorelix, a GnRH antagonist. To assess the specificity of [^{18}F]FMDHT towards ARs, a separate group of animals was pretreated with a large dose of androgen before the [^{18}F]FMDHT injection.
Results The in vivo biodistribution results show selective uptake of [^{18}F]FMDHT in the prostate that ranged from 0.46+0.10 %ID/g at 1 h to 0.59+0.16 %ID/g at 3 h with prostate to muscle ratio ranging from 8.06+2.46 at 1 h to 18.81+4.90 at 3 h.
Conclusions These in vivo distribution studies document a high selectivity and specificity of [^{18}F]FMDHT towards AR rich tissues and suggests that [^{18}F]FMDHT may be a useful in vivo PET imaging ligand.

S. Garg (✉) · A. Doke · K. W. Black · P. K. Garg
PET Center, Department of Radiological Sciences,
Wake Forest University Health Sciences,
Medical Center Blvd,
Winston Salem, NC 27157, USA
e-mail: pgarg@wfubmc.edu

Keywords F-18 FMDHT · Androgen receptors · Prostate cancer · Tissue distribution in rats · Positron emission tomography · 7-α-fluoro-17 α-methyl-5-α-dihydrotestosterone

Introduction

Prostate cancer is a leading non-skin cancer in America. More than 210,000 men will be diagnosed with prostate cancer this year and about 27,000 men will die of this disease each year. If the prostate cancer is diagnosed in the early stages, a 5-year disease-free survival rate from this cancer is very high. Therefore, developing a reliable diagnostic test for early detection and localization of prostate cancer is important.

Androgen receptors (AR) play a significant role in the normal growth, cell differentiation, and maintenance of prostate epithelium. Both the primary and metastatic prostate cancers express AR to similar extent [1]. The prostate cancer growth depends on AR-signaling that activates over-expression of AR-regulated genes such as prostate specific antigen (PSA) and others [2]. Because of its direct relevance to prostate cancer growth, the current diagnosis relies on rising PSA levels as an indicator for prostate cancer and disease progression. Despite its routine use in the clinic, this method is not reliable and underscores the need to develop a more accurate and reliable diagnostic tool. Therefore, developing an AR-based ligand for the diagnosis of prostate cancer has been the goal of many laboratories including ours.

Testosterone and 5α-dihydrotestosterone (5α-DHT) are two major endogenous androgens that bind specifically to the AR. Amongst the two, the 5α-DHT exhibits higher

potency as an androgen. Therefore, we focused our attention on utilizing the structural motif of 5α-DHT into our molecule. In the past, we developed 7α-fluoro-17α-methyl 5α-dihydrotestosterone ([^{18}F]FMDHT) as a ligand for AR-mediated PET imaging of prostate cancer [3, 4]. Earlier, Labaree et al. [5] reported the synthesis of 7α-fluoro-17α-methyl 5α-dihydrotestosterone (FMDHT), a non-radioactive analogue. This compound showed enhanced binding to AR when compared to 5α-DHT and other related structural analogues. In addition, binding of FMDHT to other receptors was negligible and exhibited a high specificity towards the AR. To explore its utility as a PET imaging agent for ARs, we radiolabeled this probe with fluorine-18 and assessed its in vivo distribution and specificity to target tissues. In our preliminary in vivo evaluations, we reported [^{18}F]FMDHT showing preferential uptake in AR positive tissue and a low uptake in the normal tissues [3]. Despite encouraging biodistribution data obtained from rats castrated using the diethylstilbestrol (DES) via the chemical castration method, it provided suboptimal and inconsistent results. It is likely that DES-induced castration used in those studies may have provided incomplete and unreliable suppression of testosterone in those animals. Therefore, we reassessed the in vivo properties of this ligand agent utilizing the rats castrated via a newer approach, which utilizes the testosterone suppression capability of GnRH antagonists to attain castration in rats. The role of GnRH agonists and antagonists in desensitizing pituitary GnRH receptors and inhibiting gonadotrophin and testosterone secretion is well documented [6, 7]. Herein, we report in vivo distribution of [^{18}F]FMDHT in rats pretreated with cetrorelix, a GnRH antagonist.

Materials and methods

All reactions were carried out under an inert atmosphere with dry solvents, under anhydrous conditions, unless otherwise stated. Reagents and solvents were purchased from commercial suppliers and were used without further purification. Cetrorelix was provided to us by Dr. Richard Hochberg (Yale University, New Haven, CT, USA) as a generous gift.

Radioactivity levels in the tissues were assessed with a Packard Cobra γ-counter. High pressure liquid chromatography (HPLC) was performed in isocratic mode with a Varian 9010 LC pump, a variable wavelength 9050UV VIS detector (Varian, Palo Alto, CA, USA) set at 254 λ and a radioisotope detector (Bioscan, Washington DC, USA) attached to Varian's chromatography software package (Varian). The HPLC system used for purification of [^{18}F]FMDHT was a C-18 reverse-phase ODS, 10×250 mm 5-μ column (Phenomenex, Torrence, CA, USA) eluted with H_2O/CH_3CN (50:50) at 3 ml/min. Quality control of purified product was performed using Varian HPLC system using a microsorb reverse phase Varian C-18 250×4.6 mm, 5-μ column eluted with H_2O/CH_3CN (50:50) at 1 ml/min. The microwave reactions were performed using a CEM Discover microwave system (CEM, NC, USA).

Radiochemical synthesis of 7-α-[^{18}F]fluoro 17 α-methyl-5-α-dihydrotestosterone (7α-^{18}F-MDHT) 2

7-β-tosyl-17 α-methyl-5-α-dihydrotestosterone (tosylate precursor; Scheme 1, Compound **1**) was used as our starting material for radiofluorination and was synthesized as we previously described with minor modifications [5]. F-18 fluorination of the tosylate precursor was accomplished using the method reported recently [3, 8] and is shown in Scheme 1. Briefly, aqueous [^{18}F]fluoride was produced using ^{18}O(p, n)^{18}F reaction on 95+% enriched [^{18}O] water with 45-μA beam current in a large volume [^{18}F]fluoride target. After irradiation, ^{18}O–H_2O bolus containing 500–800 mCi of [^{18}F]-fluoride was transferred from the cyclotron on to a QMA cartridge in the hot-cell and the O-18 water was recovered. The [^{18}F]fluoride was eluted from the cartridge using kryptofix/K_2CO_3 solution in acetonitrile. The remaining water was removed azeotropically using 2×500 μl acetonitrile as described [9]. The resultant dried [^{18}F]fluoride radioactivity was re-dissolved in 0.3 ml of acetonitrile and was transferred to a microwave reaction vessel containing a solution of 400–600 μg tosylate precursor (Scheme 1, compound **1**) in ~500 μl of acetonitrile using our remote control procedure. The reaction was performed in a microwave chemistry unit using the following settings: microwave power 300 W max, ramp time 1 min, maximum pressure 150 psi, maximum temperature 90°C, and a reaction time of 5.0 min. After the reaction time was expired, the reaction mixture was cooled to <50°C and injected onto the HPLC column as described earlier [8].

Biodistribution studies

In vivo biodistribution of [^{18}F]FMDHT was performed using Sprague–Dawley rats. The rats were treated with a GnRH antagonist (cetrorelix) to decrease serum testosterone levels. The rats were injected with 150 μg of cetrorelix subcutaneously at least 16 h before the biodistribution studies to induce castration. For the biodistribution studies, the castrated rats were injected with 20 μCi of [^{18}F]FMDHT via a tail vein injection. At 60, 120, and 180 min post-injection, the groups of five animals were killed, tissue of interest excised, weighed, and counted for radioactivity on a gamma counter. An additional group of five animals was injected subcutaneously with 5-α DHT (100 μg), 15 min before [^{18}F]FMDHT injection to block the ARs. This group of animals were labeled as the blocked group, and animals in this group were killed at 2 h post [^{18}F]FMDHT injection. Radioac-

Scheme 1 Radiochemical synthesis of [^{18}F]FMDHT using the tosylate precursor **1**

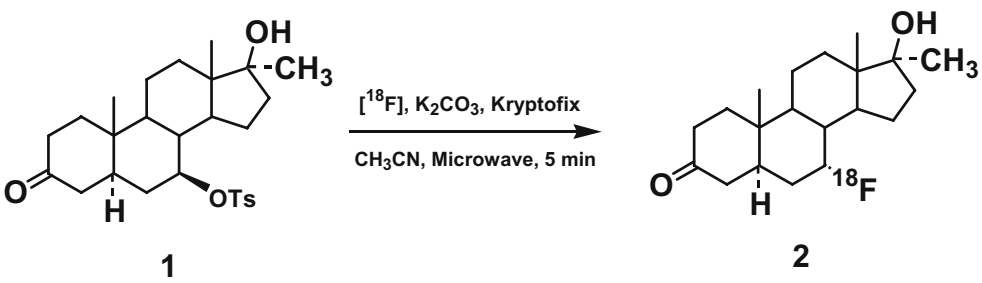

tivity uptake in various tissues was calculated as a percent-injected dose per gram of tissue (%ID/g tissue) by counting the dose standard of appropriate count rate along with the tissues.

Results and discussions

Radiochemical synthesis was accomplished as shown in Scheme 1. Reaction of [^{18}F]-fluoride/kryptofix with tosylate precursor (**1**) provided the desired product [^{18}F]FMDHT (**2**) in 24±12% radiochemical yield (EOS) using the microwave reaction. The radiochemical purity for the product was >99%. The overall synthesis time including the purification was 60–70 min. The desired product eluted at 14 min from the semi-preparatory HPLC column and at 9.7 min on a QC HPLC column using a 50% acetonitrile in water as the eluant. The apparent specific activity of [^{18}F]FMDHT ranged between 900 and 2500 mCi/μmole as determined by the radio-receptor assay [3].

In our previous studies, [^{18}F]FMDHT preferentially accumulated in tissues that express AR. Nonetheless, in repeat experiments, the reproducibility of results was marginal and inconsistent. We contemplate that incomplete castration levels achieved in those studies may have led to encouraging but ambivalent results. To achieve reliable and reproducible results, we resorted to alternate strategies to achieve testosterone suppression in these animals. Suppression of testosterone production via the hypothalamic gonadotrophin releasing hormones (GnRH) that control the secretion of luteinizing hormones (LH) and follicular stimulating hormone from the anterior pituitary gland has become common medical approach to treat androgen responsive tumors. Nonetheless, GnRH agonists cause an initial increase in testosterone secretion before complete castration is achieved [10]. On the contrary, GnRH antagonists bind competitively to the pituitary GnRH receptors and therefore do not induce LH or a testosterone surge. Mechanistically, these antagonists block the GnRH receptors and produce a fast, profound, and sustained suppression of testosterone secretion [6]. For this reason, GnRH antagonist is slowly gaining acceptance in the clinical management of prostate cancer patients [11]. Cetrorelix is one of the recently FDA approved GnRH antagonists. This agent virtually eliminates the LHRH-induced LH release from the pituitary and exhibits a downregulation of these receptors [12, 13]. A chronic as well as low dose of cetrorelix has been shown to induce a significant reduction in serum testosterone levels in rats [12, 14]. Because GnRH antagonists reduce in vivo testosterone levels quickly and reliably while not causing an initial surge in testosterone, we used this agent to castrate rats in this study. For these experiments, the animals were injected subcutaneously with 150 μg of cetrorelix and were termed as the control group. The F-18 accumulation in various tissues at 1, 2, and 3 h post-injection of [^{18}F]FMDHT is shown in Table 1.

As shown in Table 1, an initial uptake of radioactivity was observed in all the normal tissues followed by a steady washout of radioactivity with time. By 3 h-post injection, the uptake in various tissues was reduced by 20–40% of the levels attained at 1 h. A slightly different uptake and clearance pattern of F-18 was noted in the current study than that reported earlier [3]. One of the possible explanations for this disparity may be due to different mechanism of action involved with cetrorelix in vivo than for the DES to alter testosterone levels.

The persistent and high accumulation of radioactivity observed in the prostate in the current study was encouraging. The radioactivity in the prostate (the target tissue) continued to rise with time resulting in 28% more activity

Table 1 Tissue distribution of F-18 at various time points following the injection of [^{18}F]FMDHT in rats castrated using GnRH antagonist cetrorelix[a]

Tissues	% injected dose/g tissue		
	1 h	2 h	3 h
Liver	0.30±0.08	0.29±0.09	0.30±0.07
Spleen	0.07±0.02	0.04±0.01	0.04±0.01
Lungs	0.08±0.02	0.05±0.03	0.05±0.01
Kidneys	0.23±0.08	0.20±0.08	0.17±0.04
Muscle	0.06±0.01	0.04±0.02	0.04±0.01
Bone	0.38±0.25	0.47±0.27	0.45±0.21
Blood	0.08±0.02	0.05±0.02	0.06±0.01
Prostate	0.46±0.10	0.55±0.20	0.59±0.16

[a] Results are mean±SD for five animals.

at 3 h than that at 1 h. These levels were significantly higher than we reported earlier (0.55+0.2 vs 0.26+0.03 %ID/g, p=0.005) [3] and were more comparable to the levels reported for the other F-18-labeled androgen analogues [15–17]. We hypothesize that in our previous studies, the castration levels were somewhat low or incomplete, thus, resulting in equivocal tracer uptake. Despite the successful use of DES by others in achieving testosterone suppression in rats, we were unable to acquire reliable and reproducible results using this approach. One of the possible factors could be the poor solubility of DES resulting in inadequate dose delivery. Nonetheless, use of GnRH antagonist in the present study helped us achieve castration levels in rats with no difficulty.

Another significant finding from this study was that the F-18 uptake in the target tissues observed herein was similar to other androgen analogues. In addition, an overall low uptake of [^{18}F]FMDHT was observed in normal tissues. For example, uptake in the liver and lungs at 1 h post-injection was two to threefold lower for the [^{18}F]FMDHT than that reported for the 16β-F-DHT or 16α-F-MNT [15, 16]. The lower magnitude of uptake and a steady washout of radioactivity from normal tissues with time as observed in this study are advantageous. For example, the low accumulation of radioactivity in normal tissues would cause low background activity during imaging and would deliver a reduced radiation dose to the subject. The rapid washout of radioactivity from normal tissues in conjunction with rising uptake in the target tissue with time further strengthens our belief that [^{18}F]FMDHT would be a suitable ligand for its intended use.

Because steroids are metabolized rapidly in vivo, the design constraints are severe for developing novel imaging ligands that are capable of exhibiting in vivo metabolic stability along with an enhanced biological activity. For example, one of the iodinated analogues that we synthesized, 7α-iodo -17α-methyl 5α-dihydrotestosterone, had an excellent relative binding affinity for the ARs. Although, it had a high affinity for the AR, paradoxically, it concentrated poorly in the prostate in vivo. Upon further study, we discovered that while the 7α-iodinated steroid was stable in aqueous media indefinitely at 0°C, the temperature at which the receptor studies were performed, at physiological temperature of 37°C, the 7α-iodo group was rapidly eliminated. This observation stresses the importance of monitoring the in vivo dehalogenation for the newly developed radiolabeled steroids. For the fluorinated compounds, in vivo defluorination can be monitored by measuring bone uptake of the compound. Previously reported fluorinated steroids varied dramatically in their in vivo defluorination. The bone uptake for androgens incorporating F-18 in β-configuration (16β-fluoro-MNT) show a seven to ninefold higher bone uptake when compared to its α-configuration analogues [16]. For example, F-18 uptake in the bone for 16β-F-DHT, 16β-F-T, 16β-F-Mib was 4.15+2.04, 3.24+0.47 and 0.47+0.08 % ID/g, respectively, at 2 h post-injection. In contrast, radioactivity uptake for the 16α-F-MNT was only 0.28+0.24%ID/g of bone [16]. Based on the structure activity relationship derived from that study, the authors hypothesized that the substitution of a 17-α methyl group and an α-orientation for the fluorine atom were critically important factors in achieving in vivo stability of these molecules. We sought these two design criteria in designing our radiotracer. [^{18}F] FMDHT incorporates the desirable 17-α methyl group, and the fluorine atom was placed in an α-orientation at position 7 to achieve enhanced molecular stability towards in vivo metabolism. When compared with other androgens, [^{18}F] FMDHT showed resistance to in vivo defluorination (Fig. 1). The bone uptake for [^{18}F]FMDHT was 0.38+0.25 and 0.47+ 0.27 %ID/g of bone at 1 and 2 h, respectively (Table 1), values much lower than majority of the androgen analogues. The resultant low defluorination and low uptake in normal tissues for [^{18}F]FMDHT was perhaps owing to incorporated design strategies and constraints.

In castrated animals, a large fraction of ARs present on the prostate are free and unoccupied by the endogenous androgens. Therefore, these receptor sites would preferentially accumulate radiolabeled androgen, whereas the other normal tissues would remain unaffected. As expected, a rapid and high uptake of [^{18}F]FMDHT in the prostate and significantly lower accumulation in the control tissues was observed. This resulted in a favorable prostate to control tissue ratio. Improved prostate to muscle ratio with time is shown in Fig. 2. This ratio increased from 8.06+2.46 at 1 h to 18.80+4.90 at 3 h. Likewise, prostate to fat ratio also improved with time, increasing from 2.75+0.14 at 1 h to

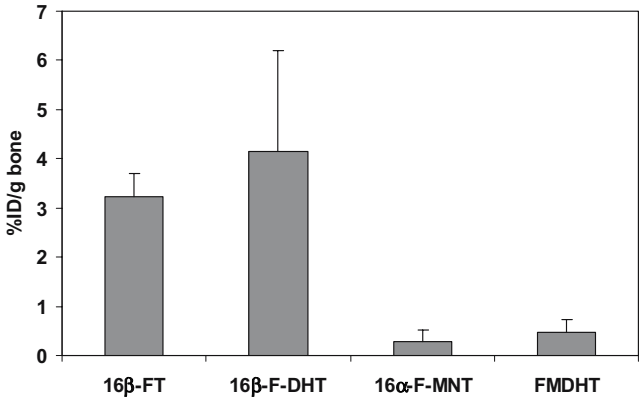

Fig. 1 F-18 uptake in the bone 2 h post-injection for various F-18-labeled androgens in castrated rats. Data for androgens other than the FMDHT is reported from [16]. A significantly low bone uptake for the analogues incorporating F-18 with α-configuration viz. the 16-FMNT and FMDHT. A seven to ninefold lower bone uptake for the FMDHT compared the a β-fluoro-DHT signifies enhanced metabolic stability of FMDHT towards in vivo dehalogenation

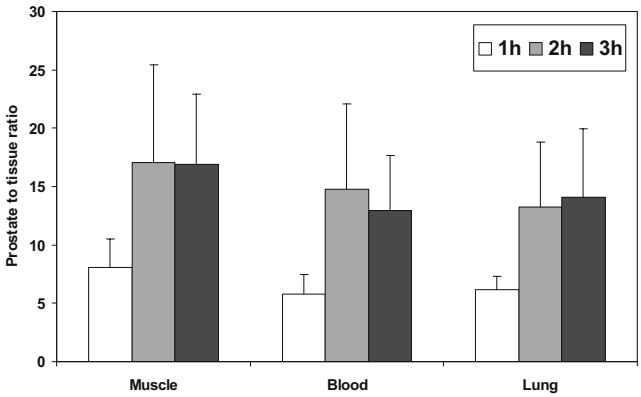

Fig. 2 The prostate to muscle ratios improved with time and reached peak level at about 2 h for most tissues. A high prostate to muscle ratio displays an excellent potential of this tracers as a useful imaging agent

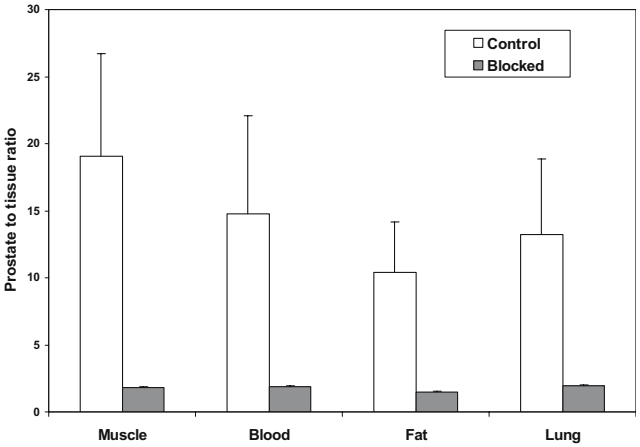

Fig. 4 Affect of androgen receptor blockade on target to normal tissue ratios in chemically castrated rats at 2 h post-injection of [^{18}F]FMDHT. Pretreatment of rats with saturating dose of 5α-DHT resulted in prostate to muscle ratio to decrease from 19 to 2. Similarly, prostate to blood, fat, and lung ratios decreased to the baseline levels on 5α-DHT treatment. These results suggest that [^{18}F]FMDHT successfully targets the tissues rich in androgen receptors. This also demonstrates that [^{18}F]FMDHT would not accumulate in the tissues lacking AR

17.08+0.62 at 3 h. Analogous results were obtained for the other control tissues including the lungs and the blood (Fig. 2). In the present study, the [^{18}F]FMDHT uptake in the prostate was similar to the levels reported for the other androgen-receptor targeting ligands [16–18].

To further assess the specificity of [^{18}F]FMDHT to AR-rich tissues, F-18 uptake in various tissues was measured before and after blocking the ARs with a large dose of 5α-DHT. To accomplish this, a group of rats was injected with ~100 μg of 5α-DHT 15 min before [^{18}F]FMDHT injection, a dose sufficient to fully occupy ARs. The animals were killed 2 h post-radiotracer injection, and the tissues were excised, weighed, and counted in a gamma counter. The F-18 uptake in the presence (block group) and absence (control group) of an AR blocking agent at 2 h post-injection of [^{18}F]FMDHT is shown in Fig. 3. In general, a reduced uptake was observed for most tissues from the blocked group, albeit to a different extent. Among other tissues, liver and

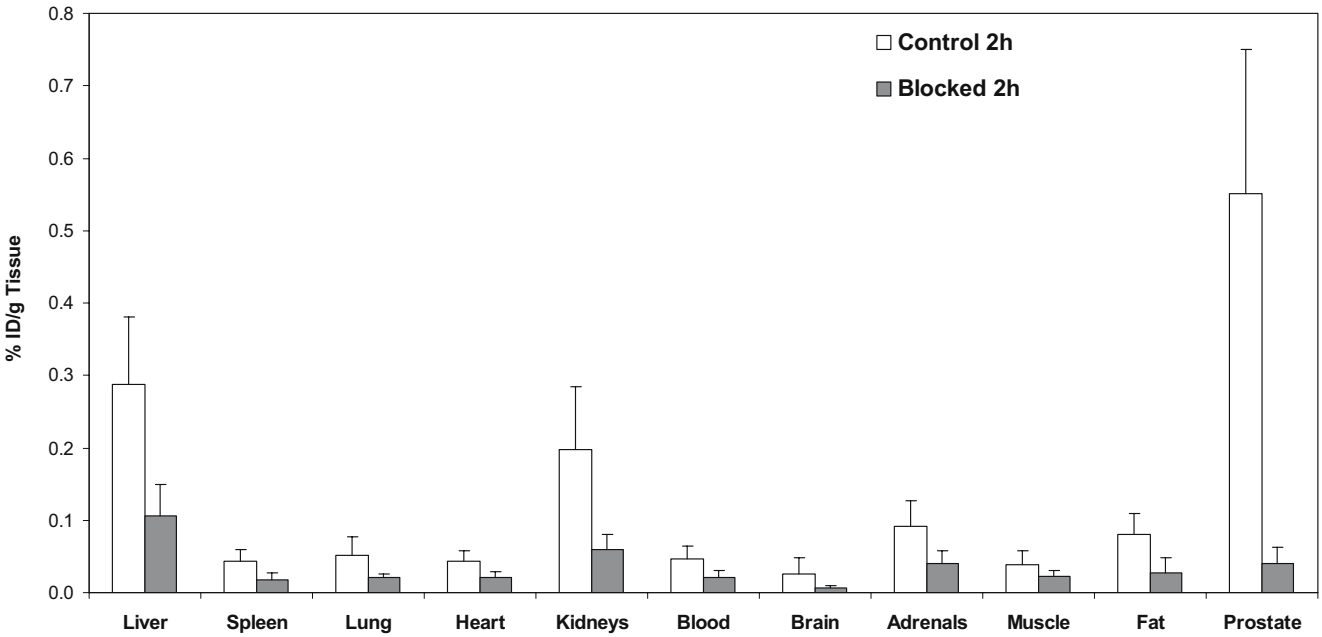

Fig. 3 Accumulation of [^{18}F]FMDHT in various tissues at 2 h post-injection of the tracer in the presence and absence of androgen receptor blocking agent DHT. DHT administration lead to a significant reduction of tracer in the prostate, a tissue known to highly express AR. A 13-fold drop in radioactivity accumulation was noticed in the prostate on 5α-DHT treatment. Liver and kidneys were the other two tissues exhibiting significantly low tracer uptake on 5α-DHT administration

kidneys were the two organs exhibiting remarkable reduction in F-18 accumulation on 5α-DHT pretreatment. Although, the initial uptake in the liver for [^{18}F]FMDHT was significantly lower than that reported for other fluorinated androgens (at 2 h: [^{18}F]FMDHT 0.29+0.09; 16β-F-DHT 0.46+0.14) [16], further reduction in F-18 accumulation on 5α-DHT treatment was interesting. A 64 and 70% lower accumulation of radioactivity was observed for the liver and the kidneys, respectively. These findings are not surprising, as it is well recognized that the liver of male rats is markedly androgen responsive and binds to androgens in a high affinity and low capacity manner [19, 20]. In addition, the kidneys and the submaxillary gland are some of the other non-sex organs that express AR [21]. Therefore, it is plausible that the marked reductions observed after 5α-DHT pretreatment reflect depleted ARs. It is implicit that liver is an organ that would metabolize and clear radiotracer from the body while retaining the radioactive metabolites as well as the receptor bound tracer, if any.

The most prominent reduction from 5α-DHT pretreatment was observed in the prostate, a tissue rich in ARs. In prostate, 5α-DHT pretreatment resulted in a 13-fold reduction of radioactivity accumulation. This marked reduction in prostate uptake resulted in a high prostate to control tissue ratio, signifying improved imaging characteristics for this radiotracer. The prostate to tissue ratio for the control and 5α-DHT blocked group is shown in Fig. 4.

It is important to note that ARs play an important role in the progression of prostate cancer in both the androgen responsive as well as the androgen refractory cancer [22] and differentiation of normal prostate from prostate cancer is a key feature of a successful diagnostic imaging tool. Although Henshall et al. [23] report altered AR expression in tumor-associated stroma, most published studies do not establish relationship between stromal AR levels and the clinical progression of the disease. Using the AR immunostaining technique, a high percent positive AR nuclear area was found in malignant epithelial cells [24]. Besides this measurement being a better predictor than the Gleason score or preoperative serum PSA levels, higher AR levels correlate with tumor growth and metastasis potential [24]. Therefore, prostate to tissue ratio noted in this study and shown in Figs. 2 and 4 has large clinical implication. A high prostate to normal tissue ratio would help improve lesion detectability of the metastatic tumors.

A high F-18 uptake in prostate and a significant washout of radioactivity in blocked animal group is another positive attribute of this tracer. The tissue distribution data from the current study expressed high affinity and selectivity of [^{18}F]FMDHT towards the target tissue. These results demonstrate high specificity and selectivity of [^{18}F]FMDHT towards AR and further strengthen the potential of this tracer.

It is important to recognize that there is a large variability between in vivo data obtained from rodent studies than that seen in the larger animals. Therefore, further studies are warranted to fully explore the potential of [^{18}F]FMDHT as a clinically useful imaging ligand.

Summary

In summary, [^{18}F]FMDHT showed a favorable tracer distribution pattern in vivo. [^{18}F]FMDHT exhibited promising in vivo properties that are suitable for PET imaging applications. Further studies with [^{18}F]FMDHT in mice bearing tumor xenografts and evaluation of its imaging characteristics using higher species is warranted to explore its full potential.

Acknowledgment This research was supported through a grant from the National Institute of Health (CA105382 to PKG). We greatly appreciate excellent technical help from Richard Chad Minton and Andrew Lynch for operating the cyclotron and for providing radiochemistry support. We also acknowledge excellent technical help from Jessica Stukes, and Holly Smith for performing the biodistribution studies.

References

1. Mohler JL, Gregory CW, Ford OH 3rd, Kim D, Weaver CM, Petrusz P, et al. The androgen axis in recurrent prostate cancer. Clin Cancer Res 2004;10:440–8.
2. Gelmann EP. Molecular biology of the androgen receptor. J Clin Oncol 2002;20:3001–15.
3. Garg PK, Labaree DC, Hoyte RM, Hochberg RB. [7a-18F]Fluoro-17a-methyl-5a-dihydrotestosterone: a ligand for androgen receptor-mediated imaging of prostate cancer. Nucl Med Biol 2001; 28:85–90.
4. Garg PK, Labaree DC, Hoyte RM, Seibyl JP, Hochberg RB. An 18F labeled steroid for androgen receptor mediated imaging of prostate tumors and metasteses. J Labelled Comp Radiopharm 1999;42:S321–3.
5. Labaree DC, Hoyte RM, Nazareth LV, Weigel NL, Hochberg RB. 7a-Iodo and fluoro steroids as androgen receptor mediated imaging agents. J Med Chem 1999;42:2021–34.
6. Salameh W, Bhasin S, Steiner B, McAdams LA, Peterson M, Swerdloff R. Marked suppression of gonadotropins and testosterone by an antagonist analog of gonadotropin-releasing hormone in men. Fertil Steril 1991;55:156–64.
7. Klingmuller D, Schepke M, Enzweiler C, Bidlingmaier F. Hormonal responses to the new potent GnRH antagonist Cetrorelix. Acta Endocrinol (Copenh) 1993;128:15–8.
8. Garg S, Nichols KB, Black K, Labaree DC, Hochberg RB, Garg PK. Improved radiochemical synthesis and biodistribution of F-18 labeled androgen; [18F]FMDHT. Mol Imaging Biol 2005;7:178.
9. Garg PK, Garg S, Zalutsky MR. Synthesis and preliminary evaluation of para- and meta-[18F]fluorobenzylguanidine. Nuc Med Biol 1994;21:97–103.
10. Dupont A, Labrie F, Giguere M, Borsanyi JP, Lacourciere Y, Bergeron N, et al. Combination therapy with flutamide and [D-Trp6]LHRH ethylamide for stage C prostatic carcinoma. Eur J Cancer Clin Oncol 1988;24:659–66.

11. Trachtenberg J, Gittleman M, Steidle C, Barzell W, Friedel W, Pessis D, et al. A phase 3, multicenter, open label, randomized study of abarelix versus leuprolide plus daily antiandrogen in men with prostate cancer. J Urol 2002;167:1670–4.
12. Pinski J, Lamharzi N, Halmos G, Groot K, Jungwirth A, Vadillo-Buenfil M, et al. Chronic administration of the luteinizing hormone-releasing hormone (LHRH) antagonist cetrorelix decreases gonadotrope responsiveness and pituitary LHRH receptor messenger ribonucleic acid levels in rats. Endocrinology 1996; 137:3430–6.
13. Lamharzi N, Schally AV, Koppan M. Luteinizing hormone-releasing hormone (LH-RH) antagonist Cetrorelix inhibits growth of DU-145 human androgen-independent prostate carcinoma in nude mice and suppresses the levels and mRNA expression of IGF-II in tumors. Regul Pept 1998;77:185–92.
14. Horvath JE, Toller GL, Schally AV, Bajo AM, Groot K. Effect of long-term treatment with low doses of the LHRH antagonist Cetrorelix on pituitary receptors for LHRH and gonadal axis in male and female rats. Proc Natl Acad Sci USA 2004;101:4996–5001.
15. Choe YS, Lidstrom PJ, Chi DY, Bonasera TA, Welch MJ, Katzenellenbogen JA. Synthesis of 11b-[18F]fluoro-5a-dihydrotestosterone and 11b-[18F]fluoro-19-nor-5a-dihydrotestosterone: Preparation via halofluorination-reduction, receptor binding, and tissue distribution. J Med Chem 1995;38:816–25.
16. Liu A, Dence CS, Welch MJ, Katzenellenbogen JA. Fluorine-18-labeled androgens: radiochemical synthesis and tissue distribution studies on six fluorine-substituted androgens, potential imaging agents for prostatic cancer. J Nucl Med 1992;33:724–34.
17. Liu AJ, Katzenellenbogen JA, VanBrocklin HF, Mathias CJ, Welch MJ. 20-[18F]fluoromibolerone, a positron-emitting radiotracer for androgen receptors: synthesis and tissue distribution studies. J Nucl Med 1991;32:81–8.
18. Brandes SJ, Katzenellenbogen JA. Fluorinated androgens and progestins: molecular probes for androgen and progesterone receptors with potential use in positron emission tomography. Mol Pharmacol 1987;32:391–403.
19. Eagon PK, Seguiti SM, Rogerson BJ, McGuire TF, Porter LE, Seeley DH. Androgen receptor in rat liver: characterization and separation from a male-specific estrogen-binding protein. Arch Biochem Biophys 1989;268:161–75.
20. Sunahara GI, Finlayson MJ, Warren BL, Bellward GD. Characterization studies of a rat hepatic cytosolic androgen-binding protein. Can J Physiol Pharmacol 1985;63:952–7.
21. Fishman RB, Chism L, Firestone GL, Breedlove SM. Evidence for androgen receptors in sexually dimorphic perineal muscles of neonatal male rats. Absence of androgen accumulation by the perineal motoneurons. J Neurobiol 1990;21:694–704.
22. Cronauer MV, Schulz WA, Burchardt T, Anastasiadis AG, de la Taille A, Ackermann R, et al. The androgen receptor in hormone-refractory prostate cancer: relevance of different mechanisms of androgen receptor signaling (review). Int J Oncol 2003; 23:1095–102.
23. Henshall SM, Quinn DI, Lee CS, Head DR, Golovsky D, Brenner PC, et al. Altered expression of androgen receptor in the malignant epithelium and adjacent stroma is associated with early relapse in prostate cancer. Cancer Res 2001;61:423–7.
24. Ricciardelli C, Choong CS, Buchanan G, Vivekanandan S, Neufing P, Stahl J, et al. Androgen receptor levels in prostate cancer epithelial and peritumoral stromal cells identify non-organ confined disease. Prostate 2005;63:19–28.